Proceedings of the ASME 2018
International Mechanical Engineering Congress and Exposition
IMECE2018
November 9-15, 2018, Pittsburgh, PA, USA

IMECE2018-86709

EXAMINING ICE STORAGE & SOLAR PV AS A POTENTIAL PUSH TOWARD SUSTAINABILITY FOR QATAR

Ibraheam Al-Aali
Columbia University
New York, NY, United States
iaa2111@columbia.edu

Vijay Modi
Columbia University
New York, NY, United States
modi@columbia.edu

ABSTRACT

Soaring electricity demand from space cooling and excellent solar photovoltaics (PV) resources are creating an opportunity for the financial viability of low-emission solutions in Qatar that can compete with existing approaches. This study examines the big picture viability of combining large utility-scale PV with decentralized building-scale ice storage for cooling in Qatar. Qatar is found to have consistently high repeatable solar radiation intensity that nearly matches space cooling requirement. A means to exploit the low installed costs of PV, combined with low cost and long lifetime of ice storage (as opposed to batteries) are examined to meet space cooling loads. Space cooling is responsible for about 65% of Qatar's annual electric load (which averaged 4.68 GW in 2016). While multiple gas prices are considered, a scenario with the current gas price of $3.33/MMBTU, a PV system of 9.7 GW capacity and an aggregate ice-storage capacity of 4.5 GWh could reduce the gas-fired power generation in Qatar by nearly 39%. Here, gas-fired generation capacity to meet current load exists and hence is not costed.

INTRODUCTION

As the demand for energy continues to increase every year in Qatar, there is a need to examine sustainable energy solutions. Two major contributors to this increase are energy-intensive water desalination and the high cooling loads from buildings. Qatar has relatively high solar insolation with few rainy or cloudy days, making it particularly attractive for exploiting solar photovoltaic technology since the solar insolation is both periodic and predictable, and the cooling loads are going to be synergistic with the insolation and air temperature. Fig. 1 illustrate the synergistic relationship of electric demand and mean air temperature during the day.

While it is desirable to use the solar PV generation without storage, cooling demands continue during the evening and night. Ice storage, as examined here is a low-cost way to store excess PV generation (or any other form of low-cost power) electricity, converted using a chiller to produce cooling for conversion of water into ice, and use the stored ice at a later point in time for cooling. Ice storage can allow as much as 0.4 MJ of cooling per kg since one takes advantage of both the sensible and latent heat of phase change from water to ice but does come with a penalty of somewhat lower chiller efficiency compared to storing cold water.

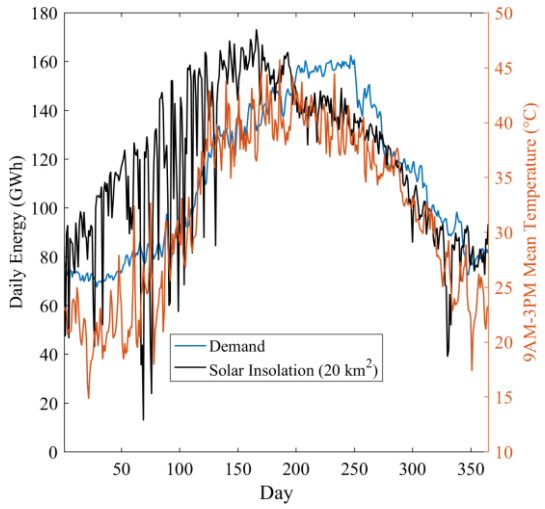

Fig. 1. Qatar's daily energy demand and daily solar insolation over 20km^2 shown in GWh, and mean of 9 AM to 3 PM ambient temperature for each day

In the literature, thermal storage has been used to increase the power grid's flexibility by handling and responding to the demand and intermittence renewables generation variability. Deetjen et al. (Deetjen et al. 2018) considered the use of thermal storage for grid wide efficiency improvements by making use of the higher cooling efficiency attained when running chillers at capacity.

Other uses include and not limited to, load shifting and peak shaving. Ice thermal storage is typically used in load shifting the cooling demand in regions with variable electricity rates or to decrease the building's required chiller's capacity. For that mode of operation, the storage would be charged during off-peak periods (typically at night) and discharged during peak periods (typically in the afternoon). Al-Hallaj (Al-Hallaj et al. 2018) studied the use of thermal storage in reducing electricity charges through peak and load shifting. Ruan et al. (Ruan et al. 2016) performed a linear

programming analysis to improve the efficiency and economics of building combined cooling, heating and power plants using thermal storage. Ruan also determined that gas and electricity charges are the main factors in determining the economic feasibility of storage.

In this study, ice storage is charged solely using the excess PV generation and discharged to attenuate the peak gas-fired generation demand and consequently gas consumption. This requires storage deployment to be strategically controlled by the utility like demand response. In a place like Qatar, the entire cost of electricity provision is borne by the national utility and hence it reasonable to assume that no additional distribution costs are incurred if the electricity is produced from solar as opposed to gas-fired turbines. Cooling is assumed to be on the customer side, either in the form of individual buildings or a cluster of buildings.

High particulate matter in the air has hindered the deployment of PV in Qatar but ongoing research is helping to evaluate and reduce the degradation due to soiling. Aïssa et al. (Aïssa et al. 2016) conducted a study on the physical properties of dust particles in Qatar and their effects on the performance of PV. Abdallah et al. (Abdallah et al. 2016) found that soiling can drop panels yield by 15% if it was not cleaned monthly in Qatar. Another study by Martinez-Plaza et al. (Martín-Pomares et al. 2017) found soiling coating to be ineffective in limiting yield drop but allowed for easier cleaning of the panels. An analysis of long-term solar potential in Qatar (Martinez-Plaza et al. 2015) found large connected PV systems to be among of the best solution in terms of inter-annual variability and long-term stability of energy generation.

In section 2 we included the assumptions made, the storage deployment strategy and algorithm employed. In section 3 we present and discuss the results of the study for three scenarios with a feasibility and sensitivity analysis for the first scenario. We conclude the study in section 4.

NOMENCLATURE

Symbol	Meaning
L_D	Hourly Electricity Demand (GWh/hr)
L_N	Hourly Net Demand (GWh/hr)
L_c	Hourly Electric Cooling Demand (GWh/hr)
L_E	Hourly Excess Load/PV Generation (GWh/hr)
I	Hourly Solar Insolation (kW/kW_p)
C	Hourly Cooling Gradient (GW/℃)
S_o	Hourly Storage Output (GWh/hr)
T	Hourly Ambient Temperature (℃)
PV_c	Solar Photovoltaic Capacity (GW)
S_{Chc}	Storage Chiller Capacity (GWh/hr)
S_c	Storage Capacity (GWh)
S_{CDL}	Storage Max Discharge Capacity (GWh/hr)
S_{CDLM}	Storage Min Discharge Capacity (GWh/hr)
η_{sc}	Storage Charge Efficiency
η_{sdc}	Storage Discharge Efficiency
η_I	Inverter Efficiency
η_{GT}	Gas to Electric Efficiency
G_c	Cost of gas ($/MMBTU thermal)
c_{PV}	Cost of Installed PV Capacity, ($/kW)
c_s	Cost of Installed Storage Capacity, ($/kWh)
c_{Chc}	Cost of Installed Chiller Capacity, ($/kW)
i	Interest Rate
t	Time

METHODOLOGY

The overall structure of the approach is to determine the combination of centralized PV generation capacity and the building-scale ice storage capacity that in combination with gas-fired generation will meet electricity and cooling demand at the same annualized cost as the current all gas-fired generation system. Cooling load is first conservatively estimated, and the rest of the electricity demand is assumed to be the non-cooling demand. PV generation is first used to meet non-cooling demand, then it is used to meet immediate cooling demand. Surplus PV is used to charge the ice-storage tank. If there is any remaining cooling demand after PV generation, then ice storage can be used to supplement it.

Qatar would likely need lower additional future gas-fired turbine capacity with the use of PV and storage, but the cost benefits of this are not counted here. Even though, Qatar's peak electricity demand has been growing at an average rate of 6.8% per year (2010-2017) suggesting benefits are immediately realized. Nor have we assumed any cost of upgrading the distribution grid. The ice storage capacity to be deployed is determined to enhance the sustainability of the grid by aiming for the highest gas reduction with zero net savings. No considerations were given to carbon taxes or costs of externalities with the use of fossil fuels. Four years of solar data were utilized to estimate uncertainties (2013-2016). Electricity demand, which is referred to as simply demand in this paper was taken as that of 2016.

Optimum deployment of ice storage is attained by maximizing storage use (charge and deploy when possible). However, the optimization strategy used in this work is developed primarily to compute the minimum required gas-fired turbine capacity to meet the demand in conjunction with PV and storage while consequently achieving maximum storage deployment. The optimum combination of centralized PV generation, building-scale ice storage, and gas-fired turbine capacity is obtained by iterating the computations with ranges of capacities. Small step sizes (<5% at most) are taken to ensure a reasonable accuracy of the optimum. The increments are made in 0.1 GW for PV_c, 0.25 GWh for S_c and $S_{Chc}/20$ for chiller capacity. Total annualized capital investment and savings in an iteration respectively,

$$c_a = (c_{PV}PV_c + c_{Chc}S_{Chc} + c_sS_c) \times \frac{i(i+1)^{yr}}{(1+i^{yr})-1} \quad (1)$$

$$s_a = 0.0034\frac{MMBTU}{kWh}\frac{G_c}{\eta_{GT}}\sum[L_D(t) - L_N(t)] - c_a \quad (2)$$

PV_c, S_{Chc}, and S_c are PV and storage chiller and thermal capacities respectively. G_c is the cost of consumed gas. In this study, we have made assumptions to simplify the problem with the expectation of not significantly compromising the intended outcome of the study. The assumptions in no order:

Gas costs and existing power generation:
- G_c at \$3.33, \$5 and \$10 per thermal MMBTU
- η_{GT} of 31% (current value)

PV:
- PV is installed fixed horizontally
- Only excess PV generation charges the storage
- PV generation is fed into the national grid
- η_I of 90%
- c_{PV} at \$700/kW [8]

Ice Thermal Storage:
- c_{Chc} at \$260/ton [9]
- c_s at \$100/ton-hr
- Distribution of coolant is not costed
- Fixed storage cooling COP of 3.4 [10]
- η_{sc} and η_{sdc} of 90%
- Storage is initially empty
- Storage is perfectly insulated
- Maximum hourly discharge rate of $S_c/3$
- Minimum discharge rate of $S_c/3000$

Financial Parameters
- Interest rate, i of 5% (current value)
- PV and storage service life of 20 years

Cost of the chiller and PV are based on current market capital prices while the cost of storage capacity was selected based on our understanding of the material used and the complexity of the manufacturing of ice storage. Operation and maintenance costs are assumed to be minimal and are ignored. For the cost of gas where operating costs are substantially higher, the price used is the effective thermal to electric price and not that of fuel alone. Finances are done for 20 years, although the storage and PV are likely to outlast that period.

The inverter is assumed to be somewhat on the higher end of efficiency. Charging and discharging efficiencies account for thermal losses during distribution with a roundtrip efficiency of 81%. The maximum discharge limit is set based on the typical performance of an ice storage operating at their maximum designed temperature difference. Minimum discharge, on the other hand, is selected to limit small discharges that would otherwise make deployment of storage cumbersome or impossible.

Cooling Load Estimation

Electric demand varies due to variation in the weather, between the time of the day, week and year, and due to other minor factors. We estimated the hourly cooling load gradient, $C(t)$, defined as the change in demand due to change in ambient temperature, from the hourly demand by least squares linear regression of demand vs. ambient temperature. The data were filtered for each specific hour for weekdays and weekend separately. We assumed all other variations are entirely due to variations in the weather and hence are the result of space cooling. A linear relationship between demand and the ambient temperature is exhibited beyond a certain temperature, termed the cooling threshold temperature. The apparent cooling threshold temperature was found to be 23°C by simple observation of the data,

$$C(t) = \frac{(k \sum L_D(t)\, T(t)) - (\sum T(t) \sum L_D(t))}{(k \sum T(t)^2) - (\sum T(t))^2} \quad (3)$$

$T(t)$ is the ambient temperature, $L_D(t)$ is the demand and k is the number of observations. Although the cooling threshold temperature is known to be lower, it cannot be effortlessly distinguished from the base load. Fig. 2 shows the cooling gradient for weekend and weekdays. From the cooling gradient, we computed the cooling demand by reasonably assuming the actual cooling threshold temperature to be 18°C. This estimates the total demand for space cooling in Qatar to be 42% (actual being near 65%). Hence the hourly cooling demand is estimated as,

$$L_c(t) = \max[C(t)(T(t) - 18°C), 0] \quad (4)$$

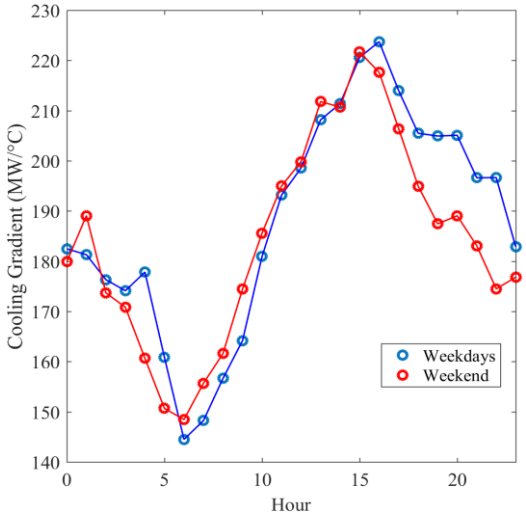

Fig. 2. Cooling load gradient for weekend and weekdays

Storage Deployment Strategy

Since ice storage could only be charged using excess PV generation, it must be either exclusively in a charging (including fully charged) or discharging (including empty) mode. In our storage algorithm, we consider each occurrence as a cycle. Each charging cycle must be followed by a discharging cycle. Discharging cycle is initiated whenever there is a lack of excess PV generation. Optimization strategy is then performed on each discharging cycle independently.

In each charging cycle, we compute the maximum storable excess solar generation, $E(m)$, that could be deployed in the following discharge cycle with any remaining stored energy from the previous cycle. To compute it, we

ensure the stored energy does not exceed the storage or chiller capacity such that,

$$E(m) = \min\left[\sum_n L_E(t_n)\eta_{sc}\left(\frac{COP}{COP+1}\right),\ S_c\right] \quad (5)$$

$$L_E(t_n)\left(\frac{COP}{COP+1}\right) \le S_{Chc} \quad (6)$$

$L_E(t_n)$ is the excess PV generation, COP is the coefficient of performance, S_{Chc} is the chiller capacity, and η_{sc} is charging efficiency. Remaining stored energy, if any, after deployment in the cycle, m, is moved to next cycle, $m+1$, and capped by,

$$\min[E_{Rem}(m),\ S_c - E(m+1)] \quad (7)$$

E_{Rem} is the remaining stored energy. Fully charging the storage in the next cycle reduces Eq. 7 to zero. Optimally, with a sufficient cooling demand and stored energy, the storage is deployed to attain a uniform net demand (after PV and storage utilization) that minimizes the required gas-fired turbine capacity in the respective cycle and consequently, the gas consumption. The optimum uniform net demand (baseline) is the average net demand if the storage was completely utilized,

$$b(m) = \max\left[\frac{\sum L_N^*(t_z) - E(m)\eta_{sdc}}{|L_N^*(t_z)|}, 0\right] \quad (8)$$

For all t_z that ensure non-negative net demand,

$$L_N^*(t_z) \ge \frac{E(m)\eta_{sdc}}{|L_N^*(t_z)|} \quad (9)$$

Where $L_N^*(t)$ is intermediate net demand, which represents the net demand after direct PV generation utilization,

$$L_N^*(t_z) = max[L_D(t_z) - PV_c I(t_z)\,\eta_I, 0] \quad (10)$$

$|\ |$ is an operator that represents the length of a vector, subscript z is the vector indexing element for the respective cycle, and η_I and η_{sdc} are the inverter and storage discharge efficiencies respectively. Here, since the deployment depends on the forecasted weather and consequently the cooling demand, we assume the ambient temperature and solar insolation can be perfectly forecasted at most a week ahead which is possible in a place like Qatar with a highly cyclic and predictable weather. We then continuously deploy the storage for the first hour and re-optimize for the remaining hours of the cycle. The matrix form of the baseline,

$$B\left(L_N^*(t_z) \ge \frac{E(m)\eta_{sdc}}{|L_N^*(t_z)|}\right) = b(m) \quad (11)$$

And,

$$B\left(L_N^*(t_z) < \frac{E(m)\eta_{sdc}}{|L_N^*(t_z)|}\right) = L_N^*(t_z) \quad (12)$$

For cases when the computed discharge was greater than the discharge limit or the cooling demand, the baseline vector is adjusted to limit the discharge by the minimum of baseline, discharge limit, and cooling demand, such that:

$$B(t_z) = L_N^*(t_z) - min[b(m), \eta_{sdc}S_{CDL}, L_c(t_z)] \quad (13)$$

To maximize deployment and consequently gas reduction, in the last ≤168 hours before the following charge cycle, we make a final adjusts to each element of the vector $B(t_z)$ so that all stored energy is utilized, $[\sum L_N^*(t_z) - B(t_z)]\frac{1}{\eta_{sdc}} = E(m)$, or storage was deployed to its maximum potential or met all the cooling demand, $B(t_z) = min[S_{CDL}, L_c(t_z)]$, therefore,

$$B_{new}(t_z) = min[\sum L_N^*(t_z) - B(t_z), \eta_{sdc}S_{CDL}, L_c(t_z)] - (L_N^*(t_z) - B(t_z)) \quad (14)$$

The discharged energy by ice storage is then simply the reduction in intermediate net demand, $L_N^*(t_z)$ to net demand, $L_N(t_z)$ or $B(t_z)$,

$$S_o(m) = L_N^*(t_z) - L_N(t_z) = L_N^*(t_z) - B(t_z) \quad (15)$$

We define storage flexibility as the ability of storage to modulate its output at any given time. The definition is parameterized by computing the mean storage output over the time the storage could be utilized (no excess PV generation):

$$f = \frac{\sum S_o(t_s)}{8760 - |L_E(t_s)|} \quad (16)$$

For all t_s in which $L_E(t) = 0$. Since both, the installed PV and storage capacities are subject to variability, they cannot be completely considered as firm capacities in the grid. We use a commonly used metric, capacity credit, to evaluate the endogenous capacity of installed renewables:

$$CC = \frac{\max[L_D(t)] - \max[L_N(t)]}{PV_c} \quad (17)$$

RESULTS & DISCUSSIONS

We considered scenario 1 as the primal scenario and we discussed it in greater depth than either scenario 2 or 3. In scenario 1, we analyzed efficiency metrics and endogenous capacity of the system. We also examined the characteristics and behavior of storage operation as the capacity is increased. For scenario 2 and 3, we addressed the effects of gas price on the optimum and the key differences in the operation of storage compared to scenario 1. We then show the results of the feasibility study conducted on scenario 1 considering the spatial limitations in Qatar. Lastly, we show the outcome of the sensitivity analysis performed on scenario 1 optimum.

Analysis Outcome – Scenario 1

The first scenario we considered is the current gas price of $3.33/MMBTU in Qatar. The algorithm was executed

for PV capacity range of 0-12 GW and aggregate storage capacity range of 0-5 GWh. Box plot for capacities range at the optimum using the 4 years of solar data is in Fig 3.

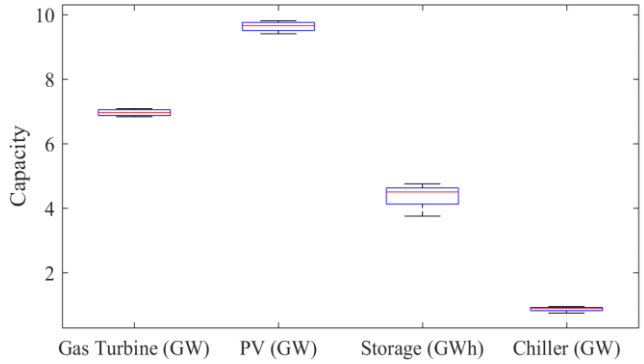

Fig. 3. Scenario 1 optimum range of gas turbine, PV, storage and chiller capacities using 4 years of solar data

The mean optimum system which is the averaged of optimum capacities from the 4 years of solar insolation data were determined to be 9.7 GW of PV, aggregate ice storage capacity of 4.5 GWh and 0.9 GWh of chiller capacity. There were small variabilities with the gas-fired turbine and PV capacities (~6-8%), however, the storage size and chiller capacities varied considerably (~28%). This suggests, although the fluctuation in solar insolation each year did not considerably impact the optimum PV capacity, it had considerable effects on the operation of the storage. This considerable variation is attributed to the PV capacity being only 30% higher than peak demand making it more prone to variation in excess PV generation. However, due to the significant difference in the cost of capital between PV ($6.72bn), ice-storage ($0.45bn) and chiller ($0.19bn), skewing the investment in favor of more storage could enhance the reliability of storage operation for a slight increase in investments.

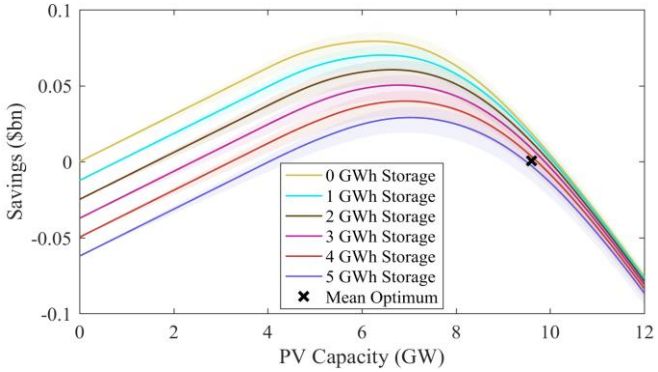

Fig. 4. Annualized savings for 0-5 GWh storage capacity with optimum chiller capacity at each point

Annualized savings for the considered PV and storage capacities range are presented in Fig. 4. Shaded regions for each curve represent the bounds of the output due to a year to year variation in solar insolation using 4 years of data from 2013-2016. This approach is used in all the figures shown. PV with no storage yields the highest savings, which explains the high PV-to-storage investment ratio of 10.1. The addition of ice storage lowers the savings in exchange for higher utilization of PV generation. Since we are aiming for the highest sustainability, the later was favored. Currently, the average cost of produced energy in Qatar is around $0.037/kWh. In this system with no net savings, the cost benefit from the reduction in gas consumption is diverted into investment in PV and storage capacities. The cost of energy produced was $0.037/kWh from gas-fired generation, $0.034/kWh is from PV generation ($0.029/kWh before curtailment) and $0.050/kWh using ice-storage.

Since power generations in Qatar exclusively use natural gas, the demand met by PV generation is the same as gas consumption and CO2 emissions reductions. The demand met by PV generation (directly and non-directly) is shown in Fig. 5. Under 4 GW of PV capacity (below average demand of 4.68 GW) all the PV generation is directly utilized with barely any excess PV generation. Above 5 GW (above average demand) PV begins to generate excess energy and the demand met becomes a weak function of ice-storage capacity. However, above 8 GW of PV capacity (above peak demand of 7.3 GW), excess PV generation become more frequent which allows the storage to be utilized more frequently and thus, makes the demand a stronger function of storage capacity. At the optimum, demand met by PV generation was 39.65% of which 2.52% was supplied by ice-storage. Although 2.52% appears to be small, it was delivered by a mere ~0.7hrs worth of storage which promotes the use of ice-storage in a place like Qatar. Since the capital cost of PV is far greater than storage or chiller, moving toward higher PV capacity reduces the difference in savings among the considered range of storage capacities (can be seen in Fig. 4) while the difference in demand met by PV generation grows (can be seen in Fig. 5).

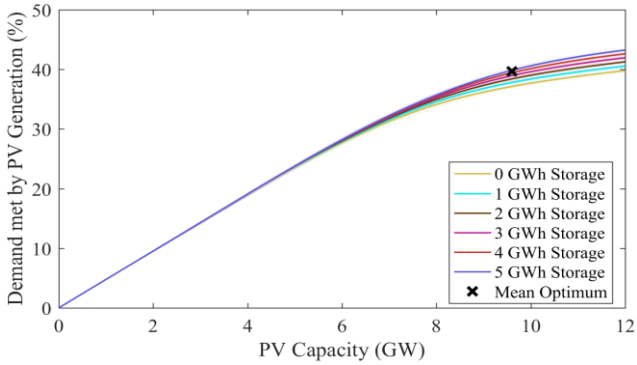

Fig. 5. Demand met by PV generation with storage which is also gas consumption and CO2 emissions reduction

Fig. 6 show the capacity factor and lost PV generation for the considered range of PV and storage capacities. Lost PV generation includes losses due to storage

and inverter efficiency and energy consumed by the chillers. Inverter losses alone account for 10% of the losses. The maximum capacity factor is 22.3% in Qatar for fully utilized horizontally laid PV panels. At high PV penetration, the capacity factors drop as some of PV generation is curtailed. The storage can boost the capacity factor by utilizing the otherwise would be curtailed excess PV generation. At the optimum, the PV capacity factor was 19% with an increase of 0.5% from sole direct PV generation. Lost PV generation was 15.28% mainly due to the installed PV capacity being only slightly higher than the peak demand. The difference in the lost generation between with and without storage increases with PV capacity as the additional PV generation is curtailed.

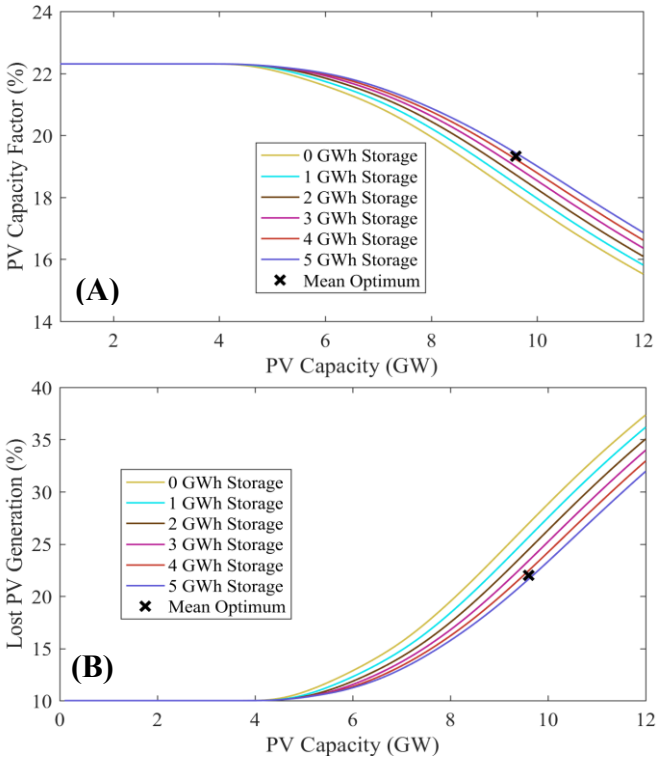

Fig. 6. PV efficiency metrics: A) capacity factor; B) Lost generation due to curtailment, storage and inverter losses, and energy used by chillers to make ice

The minimum required gas-fired turbine capacity and capacity credit for a range of PV and storage capacities are shown in Fig. 7. The variations were by far higher than any other considered parameter. The variability is reduced when PV penetration in the grid is increased at the expense of higher curtailment and capital investment. Thus, a higher PV capacity might be necessary to reliably reduce gas-fired turbine and perceive more of installed renewable capacity as firm capacity. At the optimum, the peak gas-fired turbine capacity was reduced on average by 325 MW which is about 4.5% in reduction. The capacity credit was 3.66%.

In Fig. 8 we show six storage characteristics: storage flexibility, storage capacity factor, average charge residency, max storage deployment, and storage charging and discharging frequency. Storage flexibility was defined as the storage ability to provide an output when it could be utilized which measures the storage ability to absorb the fluctuations from demand and PV generation. At the optimum, the flexibility was 0.15 GW/hr with a maximum discharge of 1.01 GW (limited by discharge limit).

Average charge residency time on basis of first in first out exhibit a decaying function behavior. When the PV capacity was small, charging cycles became sparser as excess PV generation is less frequent. This influence the range of time in which the storage could be utilized. The frequency of charging and discharging per year can be viewed in Fig. 8 (e) and (f). At the optimum, the average charge residency was 10 hours which suggests a daily operation of storage. Energy is stored during the day and effectively emptied overnight. This can be validated when looking at the storage capacity factor in Fig. 8 (c), which represents the ratio of the effective number of full discharge cycles in a year to the maximum of 365 cycles/yr. Lack of cooling in Winter limits the capacity factor to around ~0.84. At the optimum, the capacity factor was 0.63.

Despite being counter-intuitive, the charging frequency for 1 GWh of storage was slightly higher than that of 5 GWh. That is because the chiller capacity is sized with respect to storage capacity which limits the charging speed. Effect of chiller capacity decreases with bigger storage capacity and ultimately becomes negligible.

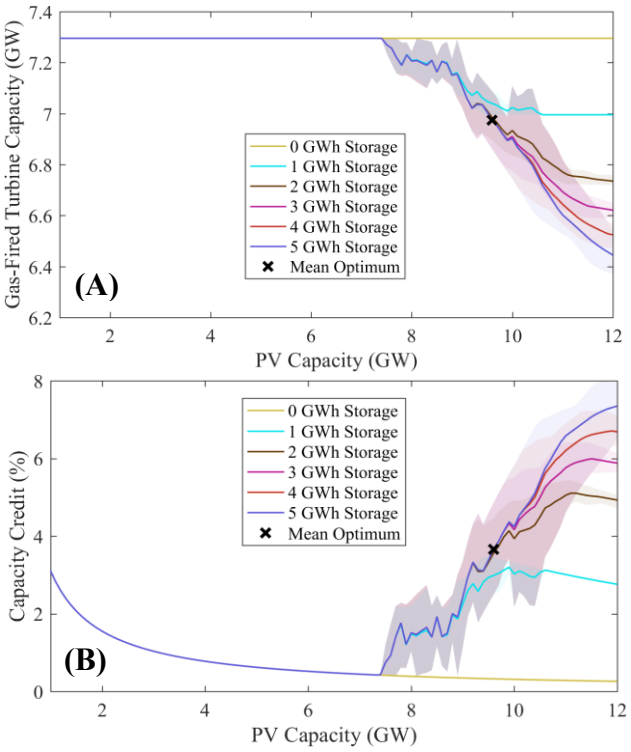

Fig. 7. Effects on gas-fired turbine capacity A) peak demand; B) Capacity credit

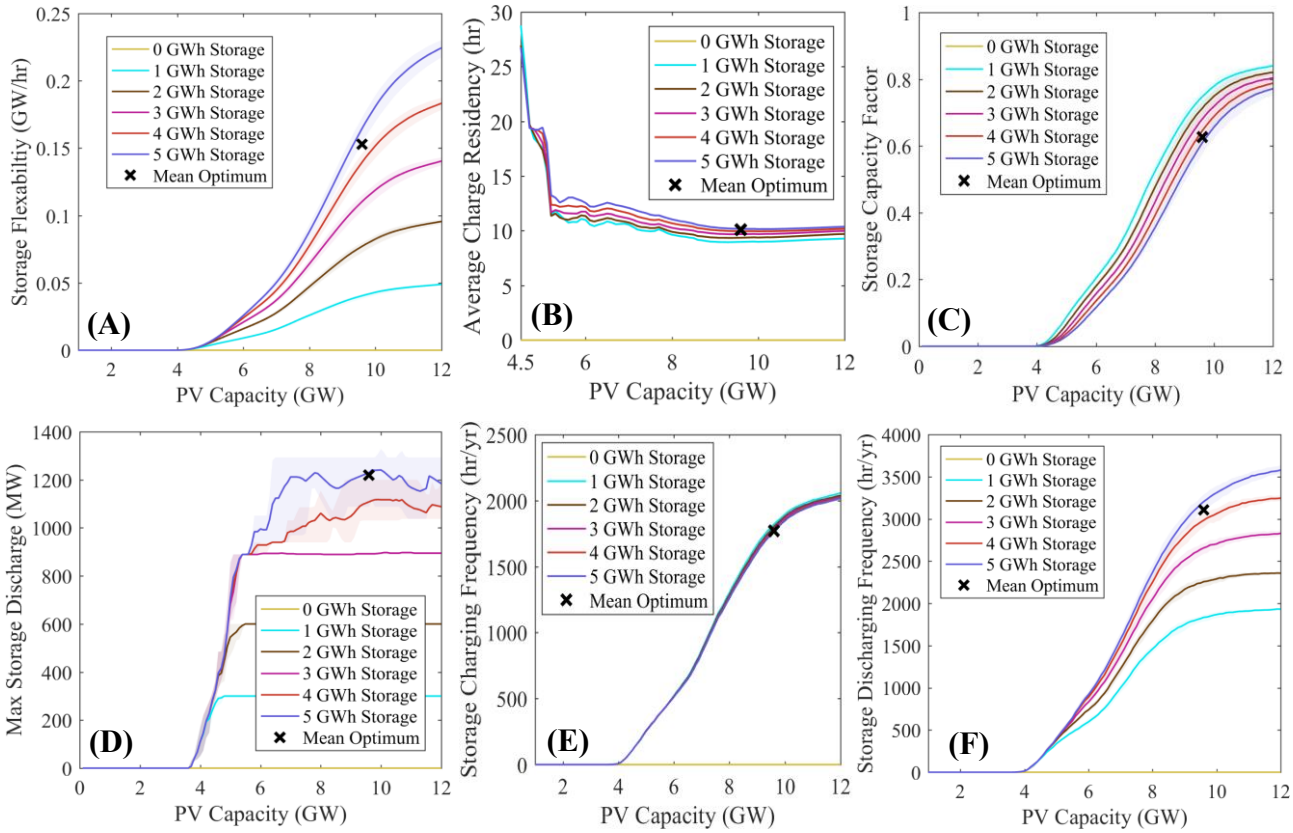

Fig. 8. Storage characteristics: A) Storage Flexibility; B) Mean Charge Residency; C) Storage Capacity Factor; D) Maximum Storage Discharge; E) Storage Charging Frequency; F) Storage Discharging Frequency

Daily maximum and total supplied energy for the optimum case are shown in Fig. 9 using 2016 solar insolation data. Almost all the reduction in the use of gas-fired generation is due to direct PV generation utilization. The storage benefited from the cheap excess PV generation to further reduce gas consumption. Synergetic relationship of cooling demand with temperature and insolation allowed for the reduction of needed gas-fired turbine capacity by around 325 MW. This is a further benefit that was not accounted for in the annualized savings. On the other hand, in the winter, deficiency of cooling demand resulted in less storage utilization. Load profile for the first week in summer (June 21st-27th) and winter (December 21st-27th) for the optimum is shown in Fig. 10 using 2016 solar data. In the summer, there were enough cooling demand and excess PV generation to allow the algorithm to achieve the expected uniform response despite not operating during the entire night. The storage is utilized around sunset till shortly after midnight. It is due to

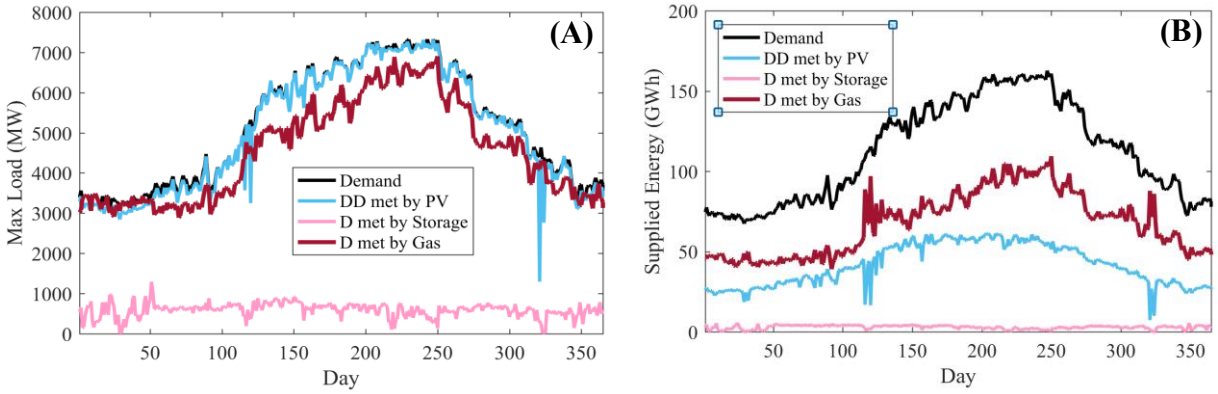

Fig. 9. Optimum system behavior for Scenario 1. A) Daily maximum values for demand, demand directly met from PV (DD met by PV), demand met by storage (D met by Storage) and demand met by gas (D met by Gas); B) Daily Energy Demand and that supplied by PV, storage and gas

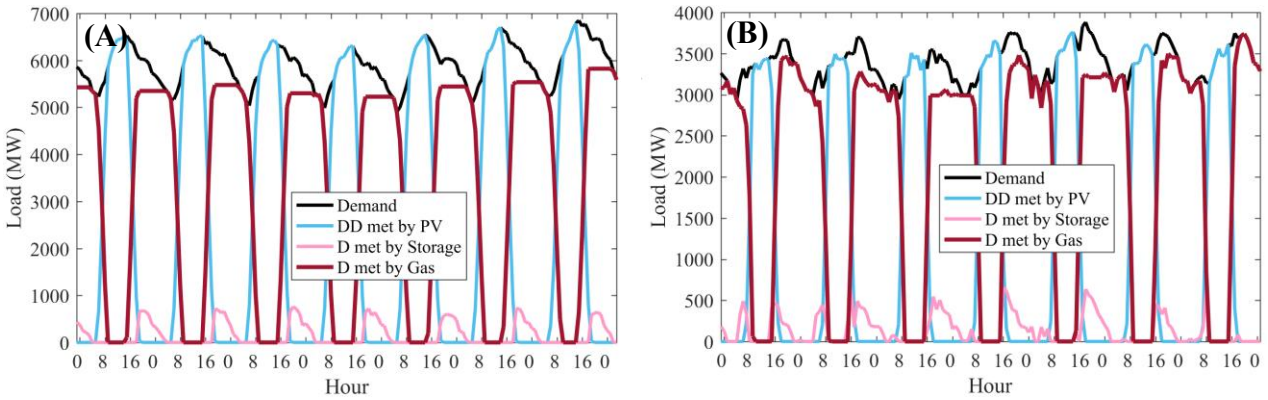

Fig. 10. Hourly load profile for demand, demand directly met from PV, demand met by storage and demand met by gas, storage and gas for the first week in A) summer and B) winter for scenario 1

fact that the temperature drops overnight and subsequently the cooling demand that allowed the storage to achieve the uniform response. In both seasons, the deployment was skewed toward early evening because the second peaks typically occur at around 7 pm.

Analysis Outcome – Scenario 2

In the second scenario, we considered a higher gas to electricity price of $5/MMBTU in Qatar. The price is going to increase when the government completely lifts subsidies when current contracts with power producers expire. The algorithm was executed for PV capacity range of 0-20 GW and storage capacity range of 25-35 GWh. Box plot of optimum range can be seen in Fig. 11. The range of storage capacity was narrowed by executing the algorithm with a larger step size to reduce the computational time.

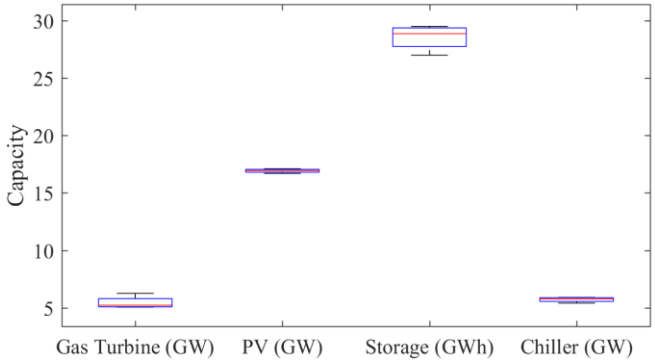

Fig. 11. Scenario 2 optimum range of gas turbine, PV, storage and chiller capacities using 4 years of solar data

Less variability in the optimum is observed in this scenario and it is attributed to the increased PV and storage capacities at the expense of higher curtailment. The mean optimum point for scenario 2 was found to be 17 GW of PV, an aggregate ice-storage capacity of 28.25 GWh and 5.65 GW of chiller capacity. The capital investment was $12.7bn for PV, $2.9bn for ice-storage and $1.4bn for the chiller. This represents an investment ratio of PV-to-storage of 2.95 which is substantially less than scenario 1's PV-to-storage investment ratio of 10.5. A higher price of gas to electricity led to an increase in investment in PV and storage. However, since PV already met all the demand during sunlight hours, moving toward higher storage capacity was necessary to further benefit from the excess PV generation and consequently reduce gas consumption during the night. A plot of the annualized savings and demand met by PV generation is shown in Fig. 12 and 13 respectively.

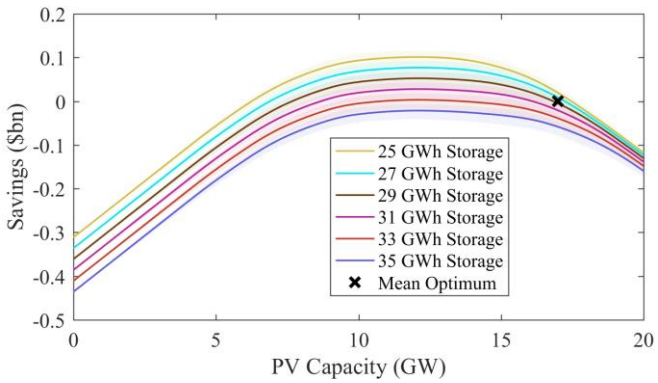

Fig. 12. Annualized savings for 25-35 GWh storage capacity with optimum chiller capacity at each point

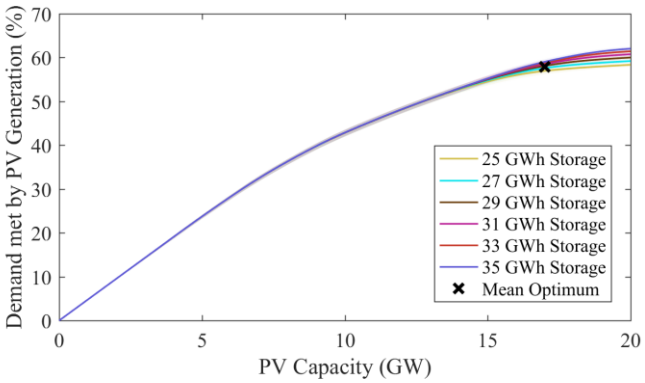

Fig. 13. Demand met by PV generation (directly and storage) which is also gas consumption and CO2 emissions reductions

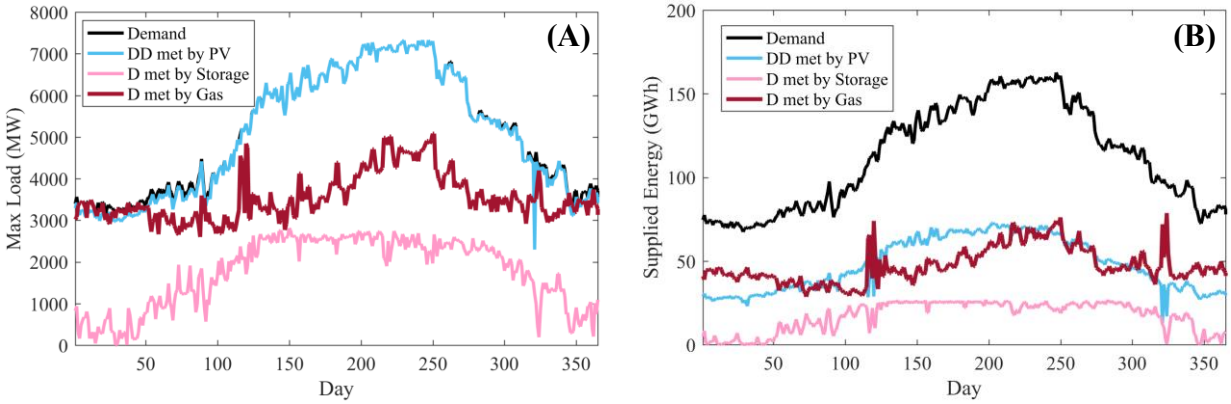

Fig. 14. Optimum system behavior for Scenario 1. A) Daily maximum values for demand, demand directly met from PV (DD met by PV), demand met by storage (D met by Storage) and demand met by gas (D met by Gas); B) Daily Energy Demand and that supplied by PV, storage and gas

As shown, 57.93% of the demand is met by PV generation, up from 39.65% for scenario 1. Storage capacity factor was 0.6 (near maximum for this capacity). Storage flexibility was 1.07 GW/hr ($1/7^{th}$ of the grid capacity) and max discharge rate was 2.8 GW. Due to the large storage capacity, only 35.54% of PV generation is lost which is only slightly higher than scenario 1. For this scenario, cost of energy produced was at \$0.055/kWh from gas-fired generation, \$0.041/kWh is from PV generation and \$0.055/kWh using ice-storage.

Daily max and total supplied energy for the optimum are shown in Fig. 14 using 2016 solar insolation data. A significant increase relative to scenario 1 in demand met by storage is observed. Ice storage supplied almost 20% of the daily total demand while only operating from evening to sunrise with a maximum discharge rate of near 3 GW. The installation of such capacity reduced the required gas-fired turbine capacity by 1.87 GW (CC of 11%). As previously stated, the cost of gas-fired turbine capacity is not coasted. For places that are yet to build its energy infrastructure, the inclusion of this cost will only skew the optimum toward higher renewable installations.

Load profile for the first week in summer and winter for the optimum using 2016 solar insolation data is shown in Fig. 15. During the night, deployment of storage reduced the gas-fired generation demand from 5-6 GW range down to 3.5 GW which is near the baseload in Qatar. In the winter, minimal cooling demand resulted in small utilization of storage. In fact, there were little to no differences in deployment between scenario 2 and 1. The storage only reduced the total demand by 0.4 GW.

Analysis Outcome – Scenario 3

In the third, scenario we are considering an extreme case where a place has a similar cooling demand as Qatar but relies on importing liquified natural gas (LNG) to meet its demand. We expect nearby MENA countries to exhibit similar cooling demand when their demand fully develop. The considered gas price was \$10/MMBTU which is the approximate cost of LNG in 2018. The algorithm was executed for PV capacity range of 0-50 GW and storage capacity range of 45-55 GWh. Box plot for capacities range at the optimum using the 4 years of solar data is in Fig 16. The range of storage capacity was narrowed by running the algorithm with a larger step size.

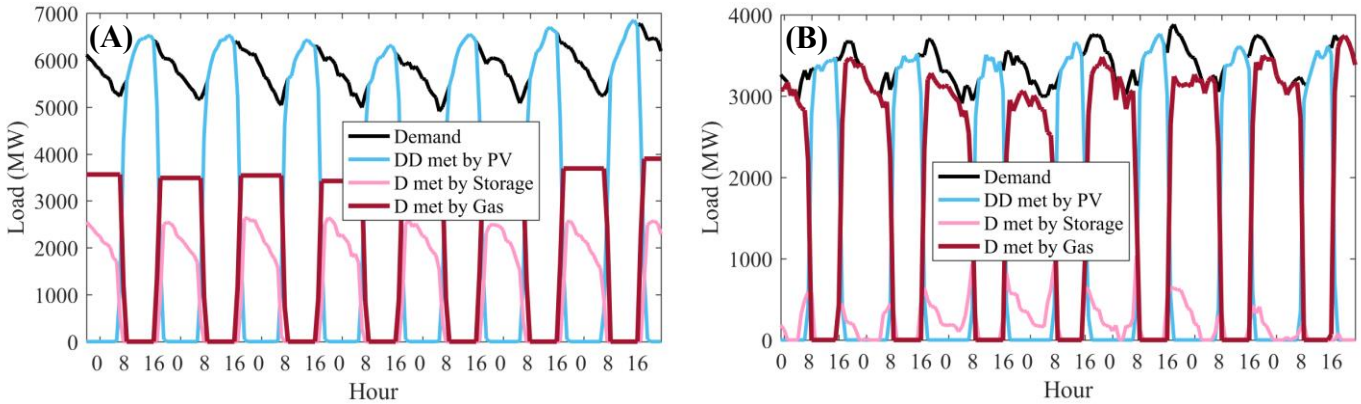

Fig. 15. Hourly load profile for demand, demand directly met from PV, demand met by storage and demand met by gas, storage and gas for the first week in A) summer, and B) winter for scenario 2

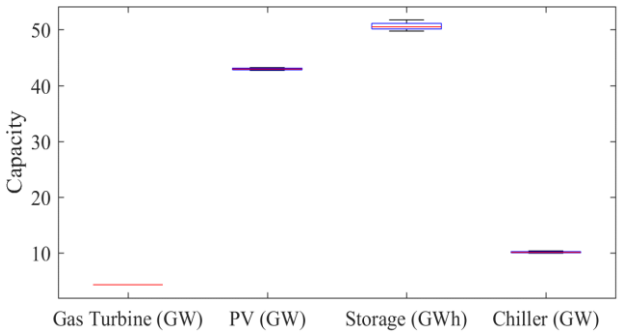

Fig. 16. Scenario 3 optimum range of gas turbine, PV, storage and chiller capacities using 4 years of solar data

The mean optimum point for scenario 3 was found to be 42.90 GW of PV, an aggregate ice-storage capacity of 50.75 GWh and 10.15 GW of chiller capacity. The capital investment was $32.2bn for PV, $5.05bn for ice-storage and $2.54bn for the chiller. This represents an investment ratio of PV-to-storage of 4.24 which is higher than scenario 2 but less than 1. The change in behavior is caused by the higher price of gas that made it worth it to invest in larger capacities until more of the cooling demand is met. However, at some point to meet more of the cooling demand, extreme investment in PV becomes necessary to charge the storage in days with low insolation. In this scenario, the storage capacity factor was 0.44, flexibility was 1.6 GW/hr and max discharge rate was 4.5 GW. Due to the large capacities, 70.17% of PV generation is lost. Cost of energy produced was at $0.110/kWh from gas-fired generation, $0.112/kWh is from PV generation and $0.075/kWh using ice-storage.

A plot of the demand met by PV generation is shown in Fig. 17. For this scenario, 67.44% of the demand is by PV generation, of which is 52.44% is met directly by PV. The demand met started to level out beyond 40 GW of PV for all considered storage capacities. This suggests the storage effectively met the entire cooling demand during the night.

Daily max and total supplied energy for the optimum are shown in Fig. 19 using 2016 solar insolation data. The installation of such capacity significantly reduced the required gas-fired turbine by 3 GW, which is the maximum possible using ice storage. At such capacity, the variability in insolation have no effects on the needed gas fire-turbine capacity and thus, the installed PV and storage capacities can be considered as firm capacities in the grid. Furthermore, in this extreme scenario, gas-fired generation daily supplied was essentially constant energy. Thus, the capacity was only needed to meet the baseload that could not otherwise be met by ice storage.

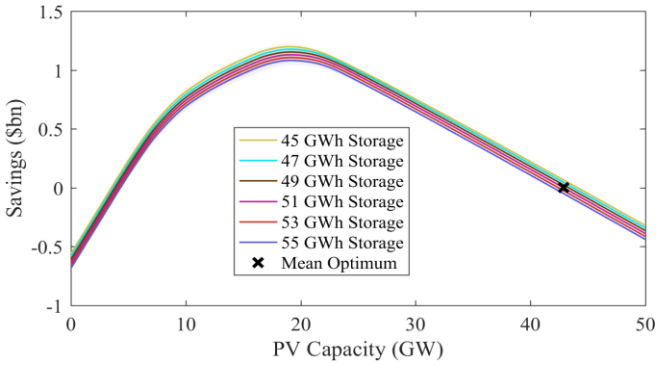

Fig. 17. Annualized savings for 45-55 GWh storage capacity with optimum chiller capacity at each point

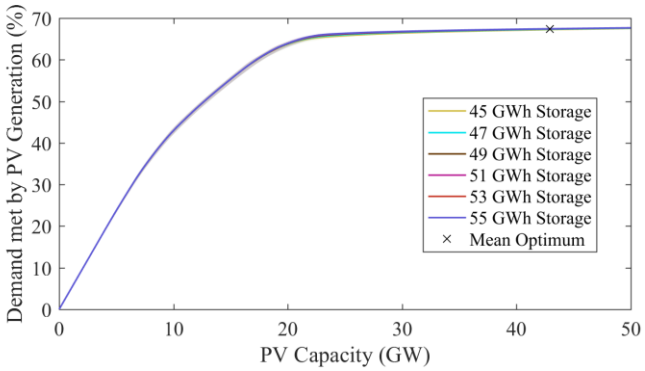

Fig. 18. Demand met by PV generation (directly and storage) which is also gas consumption and CO2 emissions reductions

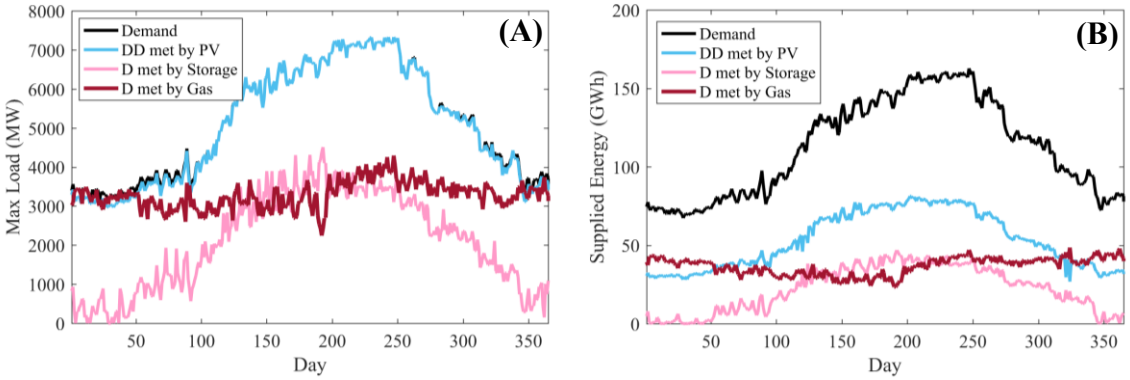

Fig. 19. Optimum system behavior for Scenario 3. A) Daily maximum values for demand, demand directly met from PV (DD met by PV), demand met by storage (D met by Storage) and demand met by gas (D met by gas); B) Daily Energy Demand and that supplied by PV, storage and gas.

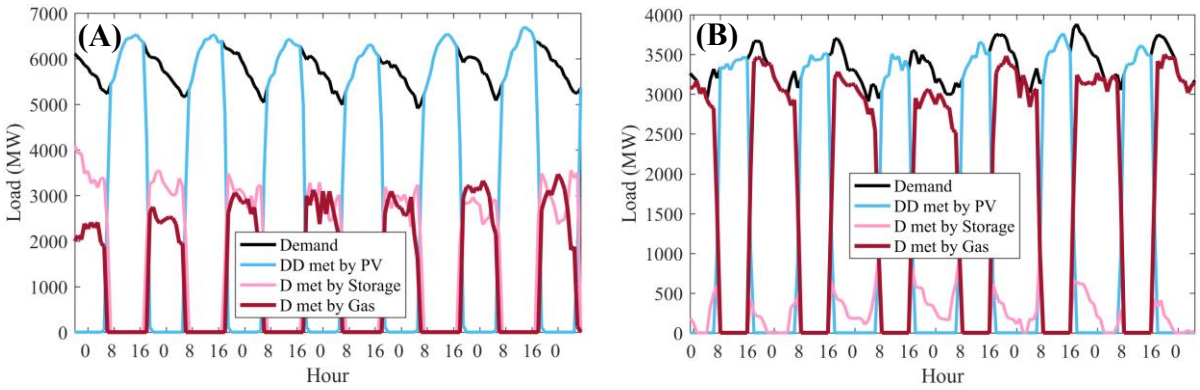

Fig. 20. Hourly load profile for demand, demand directly met from PV, demand met by storage and demand met by gas, storage and gas for first week in A) summer, and B) winter for scenario 3

Load profile for the first week in summer and winter for the optimum is shown in Fig. 20 using 2016 solar data. During the night, deployment of storage reduced the gas-fired generation demand from 5-6 GW range down to 2.5 GW, which is the baseload in Qatar. The expected uniform response no longer appears in this scenario as the stored energy was sufficient to meet all the cooling demand. Like scenario 1 and 2, in the winter, minimal cooling demand resulted in small utilization of storage. In fact, there were no differences in deployment between scenario 2 and 3.

Feasibility Study for Scenario 1

Since the considered PV and storage capacities are relatively large when considering Qatar's small land area (11, 000 km^2) and population (2.6 million), we attempted to determine the feasibility of implementing the optimum system for scenario 1 (current gas price of $3.33/MMBTU). A typical $1m^2$ PV panel has a peak capacity of 100 W which would require an area of 97 km^2 for 9.7 GW of PV capacity. Although the area is considerably large, it is feasible especially if the capacity were to be distributed in multiple locations. Fig. 21 visualize the area required relative to the size of the capital.

Ice thermal storages volume ranges from 2.4 to 3.3 ft^3/ton·hour of cooling capacity [11] which equate to about an average of 0.08 m^3/kWh of electric cooling demand for COP of 3.4. Thus, the system requires average total storage volume of 260,000 m^3. This is significantly less than the 9 million m^3 of water concrete reservoir the government is currently building to provide 7 days of strategic water storage for the expected water demand in 2026.

According to Qatar's settlement distribution 2015 census, there are about 200,000 building in Qatar [10]. The building distortion and the percent of land built for Qatar's capital, Doha is shown in Fig. 22. This suggests an average of 1.3 m^3 of ice thermal storage is required per building. However, there are already several district cooling projects around the capital with a combined thermal cooling capacity of 1 GW (~300 MW of electric cooling demand). It should be easier and more cost effective to retrofit the district cooling systems to absorb near all or all the required storage capacities especially when factoring these buildings are less limited by area (~20,000-300,000 m^2). On top of that, ice-storage requires investments in replacing the AC systems at home for it to be utilizable which adds a cost that was accounted for.

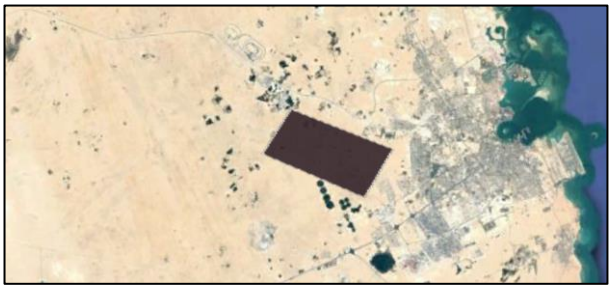

Fig. 21. Arbitrary Placed 97 km^2 polygon (Google Earth)

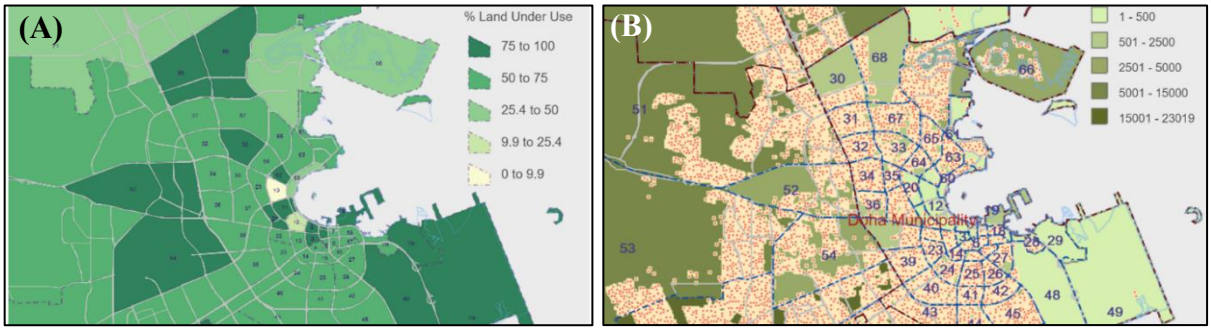

Fig. 22. Doha, Qatar's: A) Building distribution. B) Percentage of land built [12,13]

Sensitivity Analysis for Scenario 1

The prices used in this study are current market prices. Fluctuation of the cost of capital can alter the optimum capacities. A feasibility study was conducted to understand the effect of capital prices variation on the optimum point. The collective capital investment was varied by ±30% in an increment of 15%. The optimum capacities and demand met as the capital price are varied are in Fig. 23.

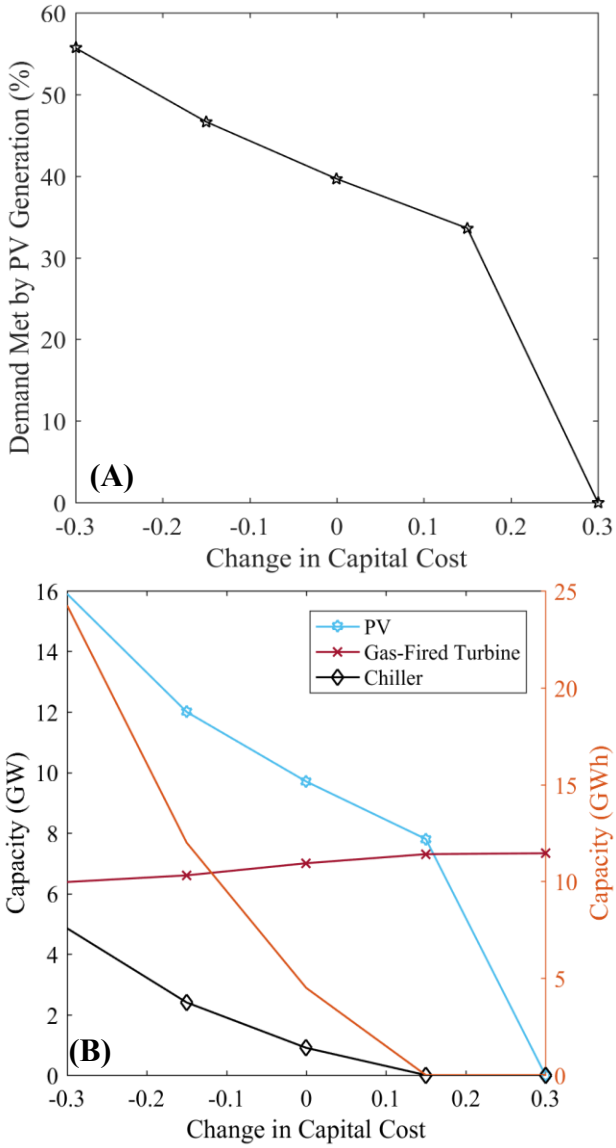

Fig. 23. Sensitivity analysis: A) Demand met by PV generation v. change in collective capital cost; B) Optimum capacities v. change in collective capital cost

Low capital prices incentivized the installation of more renewables. This pushed the demand met from 39.65% up to 57% at -30% change in capital cost. The relationship between demand met and change in capital cost appears to be near linear for the range of −30 to 20%. Increasing the capital quickly diminishes the optimum capacities reaching none at +30%. Storage appears to diminish faster by becoming financially not viable starting from +15% in the capital at a gas price of $3.33/MMBTU.

CONCLUSION

In this study, we examined the financial viability of combining large utility-scale PV with decentralized building-scale ice thermal storage for space cooling in Qatar. The storage was assumed to be charged using excess PV generation and strategically discharged and controlled by the utility to attenuate the peak electricity demand and subsequently gas consumption. Use of storage would likely lower the additional future gas-fired turbine capacity needed but it was not costed here as the capacity to meet current load exists in Qatar. For the case of Qatar with a peak demand growing at an average rate of 6.8% per year (2010-2017), this benefit is almost immediately realized.

High cooling demand that is both periodic and synergetic with solar insolation combined with consistently high solar insolation promoted the installation of PV and ice storage. As opposed to batteries, ice storage offers a long service life, low-cost of capacity and effectively non-degradable construction. Gas price was a significant factor in determining the viability of PV and ice storage. For the current gas price of $3.33/MMBTU, a system of 9.7 GW of PV and 4.5 GWh of aggregated storage capacities could reduce gas consumption by nearly 40% and peak electricity demand by 0.33 GW (4.45%). For a moderate case of gas price at $5/MMBTU, a system of 17 GW of PV and 28.25 GWh of aggregated storage capacities could reduce gas consumption by near 58% and peak electricity demand by 1.87 GW (25.6%). For the case of extreme gas from LNG at $10/MMBTU, for a place with similar cooling demand and weather as Qatar, a system of 42.9 GW of PV and 50.75 GWh of aggregated storage capacities could reduce gas consumption by 67.5% and peak electricity demand by 3 GW (41.1%) which is the maximum possible as essentially all the cooling demand was met. Capital prices also had a considerable impact on the optimum capacity. However, as capital costs are likely to remain falling especially that of PV which have been consistently falling over the past decades combined with the recovery of oil prices in 2018, the optimum capacities are likely to be higher than determined.

A limitation of this approach to sustainability is the significant spatial requirements which are aggregated when moving toward higher gas reduction. In the case of Qatar with the current gas price of $3.33/MMBTU, the optimum system claimed at least 1% of the land area (97 km^2) and 1.3 m^3 of ice thermal storage per building (total volume of 260,000 m^3).

The way we modeled this problem can be improved, we have not taken into consideration the physical and financial implications of ramping rates on gas-fired turbines nor have we addressed stability related issues of the grid with high penetration of renewables. PV and storage are expected to remain financially viable when adjusting for these factors due to strong and consistent cooling demand and solar insolation.

REFERENCES

Abdallah, A., Martinez, D., Figgis, B., and El Daif, O. (2016). "Performance of Silicon Heterojunction Photovoltaic modules in Qatar climatic conditions." *Renewable Energy*, Elsevier Ltd, 97, 860–865.

Aïssa, B., Isaifan, R. J., Madhavan, V. E., and Abdallah, A. A. (2016). "Structural and physical properties of the dust particles in Qatar and their influence on the PV panel performance." *Scientific Reports*, 6(August), 1–12.

Al-Hallaj, S., Khateeb, S., Aljehani, A., and Pintar, M. (2018). "Thermal energy storage for smart grid applications." *AIP Conference Proceedings*, 1924.

Deetjen, T., Reimers, A., and Webber, M. E. (2018). "Can storage reduce electricity consumption? A general equation for the grid-wide efficiency impacts of using cooling thermal energy storage for load shifting." *Environmental Research Letters*.

Martín-Pomares, L., Martínez, D., Polo, J., Perez-Astudillo, D., Bachour, D., and Sanfilippo, A. (2017). "Analysis of the long-term solar potential for electricity generation in Qatar." *Renewable and Sustainable Energy Reviews*, 73(March 2016), 1231–1246.

Martinez-Plaza, D., Abdallah, A., Figgis, B. W., and Mirza, T. (2015). "Performance Improvement Techniques for Photovoltaic Systems in Qatar: Results of First year of Outdoor Exposure." *Energy Procedia*, Elsevier B.V., 77, 386–396.

Ruan, Y., Liu, Q., Li, Z., and Wu, J. (2016). "Optimization and analysis of Building Combined Cooling, Heating and Power (BCHP) plants with chilled ice thermal storage system." *Applied Energy*, Elsevier Ltd, 179, 738–754.

"Solar Photovoltaic Market, Cost and Trends in EU," IEEJ, October 2006, From http://eneken.ieej.or.jp/en/data/pdf/368.pdf

"Water Cooled Chillers," FPL, Retrieved April 2018, From: https://www.fpl.com/business/pdf/water-cooled-chillers-primer.pdf

2018, "Chilled Water/Ice Storage," FVB Energy Inc., froms http://eneken.ieej.or.jp/en/data/pdf/368.pdf

Thermal Energy Storage Strategies for Commercial HVAC System, 1994, ASHRAE, from https://www.pge.com/includes/docs/pdfs/about/edusafety/training/pec/inforesource/thrmstor.pdf

Land Used Share by Areas 2015, Ministry of Development Planning and Statistics, from http://www.arcgis.com/apps/MapTools/index.html?appid=4bd74d800dbc4686a048183855367af1

Qatar Settlement Distribution 2015, Ministry of Development Planning and Statistics, from http://www.arcgis.com/apps/MapTools/index.html?appid=7d7582ba6ae54ab9a31845903616f2ad